Available online at www.rajournals.in

RA JOURNAL OF APPLIED RESEARCH
ISSN: 2394-6709
DOI:10.31142/rajar/v5i2.07
Volume: 05 Issue: 02 February -2019

International
Open Access
ICV- 74.25
Impact Factor :5.985
Page no.- 2324-2328

Mathematical Model for Lithium-Ion Intercalation into the Cathode Active Material of a Lithium-Based Cell/Battery

Sarwan S. Sandhu[1], **Clayton J. Cashion**[2], **Joseph P. Fellner**[3]

[1,2]Department of Chemical Engineering and Materials Engineering, University of Dayton, OH 45469
[3]Air Force Research Laboratory, Wright-Patterson Air Force Base, OH 45433

ARTICLE INFO

Publication Online:
27 February 2019

Corresponding Author:
Sarwan S. Sandhu

ABSTRACT

The model describing the cell discharge behavior for short cell discharge periods was developed on the basis of lithium-ion diffusion in the cathode active material as the rate limiting step. The one-dimensional model for the slab type geometry predicts the following transient behavior: lithium-ion concentration profile, lithium-ion concentration boundary layer development, electrolyte-solid cathode active material interfacial current density, and specific active material charge storage capacity as well as fractional utilization of the active material.

KEYWORDS: intercalation, lithium-ion battery, cathode active material, diffusion-limited

I. INTRODUCTION

To provide insight into the mechanistic processes governing the performance behavior of a battery/cell: $Li_{(s)}$ / electrolyte / cathode active material such as copper phthalocyanine (CuPc) or iron phthalocyanine, we have continued the process modeling activity since 2015 [1–3]. This work has also been quite helpful in the explanation of the experimental data acquired in our ongoing experimental program for the development and design of such high charge storage capacity cell cathode electrodes. The one-dimensional model described below is for the cell cathode electrode of slab geometry.

II. FORMULATION

It is assumed that at isothermal and isobaric conditions, lithium ion transfer from the electrolyte in contact with the slab of the cathode active material, such as $CuPc_{(s)}$, across the electrolyte-cathode interface at y = 0 plane is relatively much faster than the lithium ion transport in the channels of the active material. Also, it is appropriate to assume very rapid quantum mechanical adjustment of electrons in the active material while interacting with an intercalated lithium ion; thus, enabling a transferred lithium ion to occupy a most suitable active site to satisfy the condition of minimum Gibbs free energy for the stability of the cathode active material. All this and our experimentally derived information have led us to state that the lithium/lithium ion diffusion inside the active material controls the performance behavior of the cell cathode electrode due to very low lithium ion configurational type diffusivity values, e.g., 10^{-10} cm^2 s^{-1} [4]. Now, it is stated that lithium ions migrate via configurational diffusion in the active material channels as well as accumulate in it during the discharge of a lithium-based cell.

Following the “shell mass balance approach” [5], the mole balance for lithium ions is applied over the spatial element of thickness, Δy, shown in Figure 1 to obtain the partial differential equation (PDE) given below to describe the transient lithium ion concentration profile in the cathode active material.

$$\frac{\partial C}{\partial t} = \bar{D}_e \frac{\partial^2 C}{\partial y^2} \tag{1}$$

where C = lithium ion concentration in the active material, $\bar{D}_e$ = concentration mean effective diffusivity of lithium

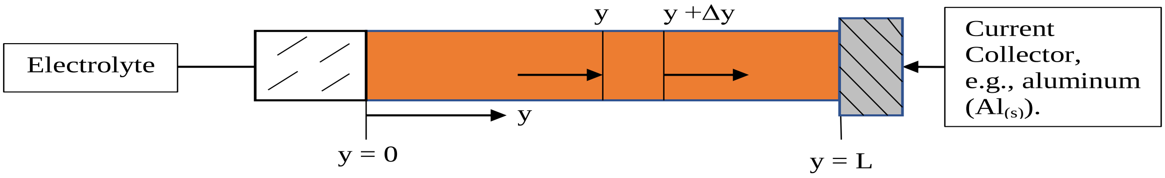

Figure 1: Slab type cathode active material electrode in contact with the cell electrolyte. Lithium ions never reach the cathode electrode current collector during the cell discharge time.

ions in the active material $= \dfrac{\int_{C_0}^{C^S} D_e\, dC}{C^S - C_0}$, C^S = lithium ion concentration in the active material at y = 0, the electrolyte – active material interface, C_0 = initial concentration of lithium ions in the active material; here, it is taken = 0, which corresponds to pure active material, $CuPc_{(s)}$, y = distance measured from the electrolyte – active material cathode electrode interface towards the electrode current collector and t represents time.

The assumed initial and boundary conditions are:

I.C. $\quad t \le 0 \quad C = C_0 = 0 \quad for\ 0 < y < L \qquad (2)$

B.C. 1 $\quad at\ y = 0 \quad C = C^S \quad for\, all\, t > 0 \qquad (3)$

B.C. 2 $\quad at\, y \to \infty \quad C = C_0 = 0 \quad for\, all\, t > 0 \qquad (4)$

The boundary condition, B.C. 2, corresponds to the situation of short time cell discharge period when lithium ions do not "see or feel" the presence of the electrode end located at the y = L plane.

Now, a dimensionless concentration, $\psi = \dfrac{C}{C^S}$ is introduced into Eq. (1) to obtain:

$$\frac{\partial \psi}{\partial t} = \bar{D}_e \frac{\partial^2 \psi}{\partial y^2} \qquad (5)$$

with initial and boundary conditions as:

I.C. $\quad \psi(y, t = 0) = 0 \qquad (6)$

B.C. 1 $\quad at\ y = 0 \quad C = C^S \quad for\, all\, t > 0 \qquad (7)$

B.C. 2 $\quad at\, y \to \infty \quad C = C_0 = 0 \quad for\, all\, t > 0 \qquad (8)$

Noting that initial and boundary conditions contain pure numbers, the solution to the PDE, Eq. (5), has to be of the form $\psi = \psi\left(y, t; \bar{D}_e\right)$. Because ψ is a dimensionless function, the quantities t, y and $\bar{D}_e$ must always appear in a dimensionless combination. The dimensionless combination of (t, y and $\bar{D}_e$) is defined as:

$$\eta = \frac{y}{\sqrt{4\bar{D}_e t}} \qquad (9)$$

This is the "method of combination of (independent) variables". The number '4' has been included so that the final solution to the PDE, Eq. (5), would appear neater.

The partial derivatives in Eq. (5) can be converted into derivatives with respect to η and simplified to the following equation:

$$\frac{d^2\psi}{d\eta^2} + 2\eta \frac{d\psi}{d\eta} = 0 \qquad (10)$$

This is a second order ordinary differential equation. The initial and boundary conditions in the dimensionless form become:

B.C. 1 $\quad at\, \eta = 0, \quad \psi = 1 \qquad (11)$

B.C. 2 $\quad at\ \eta \to \infty, \quad \psi = 0 \qquad (12)$

The first of these boundary conditions results from Eq. (3). The second, Eq. (12), represents the merging of the conditions, Eq. (2) and (4). Eq. (10) can be solved using the above boundary conditions to obtain the dimensionless concentration profile:

$$\psi = \frac{C}{C^S} = \left(1 - erf\left(\eta\right)\right) = 1 - erf\left(\frac{y}{\sqrt{4\bar{D}_e t}}\right) \qquad (13)$$

Also,

$$\psi = 1 - erf\left(\eta\right) = erfc\left(\eta\right) \qquad (14)$$

where $erfc\left(\eta\right)$ is called the complementary error function of η. The error function is a well-known function. Its numerical values are available in mathematical handbooks and nowadays in computer software programs. Using Eq (13), ψ can be calculated as a function of η and plotted versus η. The plot of ψ versus η can be employed to gain insight into the distribution of intercalated lithium in the cathode electrode active material with respect to the distance y measured from the interface between the cathode electrode active material and the cell/battery electrolyte at any time during the cell discharge operation.

In Eq. (14), the complementary error function ranges from 1 to 0. It has value of about 0.01 at $\eta = 2$. This fact is here employed to define a "lithium concentration boundary layer thickness in the cathode electrode active material", δ_C, as that distance y at which the intercalated lithium concentration, C, has dropped to a value of 0.01 C^S. That is,

$$\eta = \frac{\delta_C}{\sqrt{4\bar{D}_e t}} = 2 \qquad (15)$$

Or,

$$\delta_C = 4\sqrt{\bar{D}_e t} \qquad (16)$$

Equation (16) shows that δ_C is proportional to the square root of the elapsed time, t, measured from the moment cell discharge is initiated. Equation (16) gives a natural length scale for the diffusion of a species such as lithium ion. This distance is a measure of the extent or degree to which the lithium-ion species has penetrated into the cathode active material in time, t.

The molar flux of lithium ions into the cathode active material at the y = 0 plane at any time is given by:

$$\dot{N}_0 = \bar{D}_e \left(-\left.\frac{\partial C}{\partial y}\right|_{y=0} \right) \qquad (17)$$

Using the information from Eq. (13) in Eq. (17) and further simplification leads to:

$$\dot{N}_0 = C^S \sqrt{\frac{\bar{D}_e}{\pi t}} \quad \left[\frac{g - mol\, Li^+}{s \cdot cm_S^2}\right] \qquad (18)$$

Note that the molar flux of lithium ions into the cathode active material is inversely proportional to the square root of the cell discharge elapsed time.

The amount of lithium stored in the cell cathode active material in the cell discharge time, t, is given as:

$$n^t = \int_0^t \dot{N}_0 \, dt \qquad (19)$$

Substitution for $\dot{N}_0$ from Eq. (18) into Eq. (19) and further simplification for n^t [=] (g-moles of Li$^+$ ions)/ (cm_S^2) leads to:

$$n^t = \left[2C^S \sqrt{\frac{\bar{D}_e t}{\pi}} \right] \qquad (20)$$

The cell cathode active material is here considered to be the limiting reactant. The active material of slab geometry of thickness, L, and unit cross-sectional area has a volume, V_{activ} [=] (cm^3 / cm_S^2), given by:

$$V_{activ} = L \qquad (21)$$

The cathode electrode active material mass, m_{activ} [=] (g_{activ} / cm_S^2), is given by:

$$m_{activ} = V_{activ} \rho_{activ} = L \rho_{activ} \qquad (22)$$

where ρ_{activ} = density of the active material. The specific capacity of the active material for the storage of lithium during the cell discharge elapsed time, t, is given by $C_{sp,t}$ [=] (g-mol Li$^+$ ions or Li atoms/g active material):

$$C_{sp,t} = \frac{n^t}{m_{activ}} = \left[\left(\frac{2C^S}{L\rho_{activ}} \right) \sqrt{\frac{\bar{D}_e t}{\pi}} \right] \qquad (23)$$

The specific active material charge storage is given by:

$$Q_{sp,t} = C_{sp,t} F \qquad (24)$$

where $Q_{sp,t}$ [=] (coulomb/g active material) and F = Faraday constant = 96487 coulomb per g-equivalent. Inserting for $C_{sp,t}$ from Eq. (23) into Eq. (24) and simplifying results in, $Q_{sp,t}$ [=] (mAh/g active material), given by:

$$Q_{sp,t} = 3.0243 \times 10^4 \left[\frac{C^S}{L\rho_{activ}} \sqrt{\bar{D}_e t} \right] \qquad (25)$$

Equation (25) tells us that $Q_{sp,t}$ can be calculated as a function of the cell discharge time if the information on the values for $C^S, \bar{D}_e, L,$ and ρ_{activ} are available. If the information on the values for C^S and $\bar{D}_e$ are not available; then, from the measured values of $Q_{sp,t}$ versus t, one can determine $\left[C^S \sqrt{\bar{D}_e} \right]$ as a function of time. Then, if C^S value at the cell temperature, from an equilibrium relation between the electrolyte and the cathode active material with respect to the lithium ion concentration at a temperature, is available, $\bar{D}_e$ as a function of time, t, can be calculated from Eq. (25). This information on $\bar{D}_e$ versus t can be related to $\bar{D}_e$ versus X using the following equation for X [=] (g-mol of lithium ion stored/g-mol active material):

$$X = \left[\frac{M_{activ}}{F} \left(\int_0^t I dt \right) \right] \qquad (26)$$

where I = cell discharge current per gram of the cathode active material [amp/g] and M_{activ} = molecular weight of the cathode active material [g/g-mol]. Then, a correlation between $\bar{D}_e$ and X at a cell temperature should be developed. This work should be repeated for at least three temperatures to assess the effect of temperature on $\bar{D}_e$. Finally, an equation expressing the effect of both X and temperature, T [K], on $\bar{D}_e$; using the experimental data according to the suggestive information provided above; should be developed for the future cell active material cathode electrode design as well as for the performance analysis of an active material cathode electrode.

The fractional utilization of the cathode electrode active material is defined as

$$f_{ut,t} = \frac{\left(\begin{array}{l} \text{actual amount of lithium intercalated} \\ \text{into the cathode active material} \\ \text{during the cell discharge time, } t \end{array} \right)}{\left(\begin{array}{l} \text{maximum amount of lithium} \\ \text{which can be stored in the} \\ \text{cathode electrode active material} \end{array} \right)} \qquad (27)$$

Or,

$$f_{ut,t} = \frac{n^t}{n^t_{\max}} \qquad (28)$$

where,

$$n^t_{\max} = \left(\frac{L\rho_{activ}}{M_{activ}} X_{\max} \right) \qquad (29)$$

$X_{\max}$ = maximum g-moles of lithium which can be stored in the cathode electrode active material per g-mole of it. Inserting for n^t and $n^t_{\max}$, respectively, from Eq. (20) and (29) into Eq. (28) leads to:

$$f_{ut,t} = \left(\frac{2}{\sqrt{\pi}} \right) \left(\frac{C^S M_{activ}}{L\rho_{activ} X_{\max}} \right) \sqrt{\bar{D}_e t} \qquad (30)$$

The interfacial current density across the interface between the cell electrolyte and the cell cathode electrode active material, when the lithium diffusion in the cathode electrode active material controls its performance as well as that of the entire cell/battery, is given by:

$$i_s = \dot{N}_0 F \qquad (31)$$

Substitution for $\dot{N}_0$ form Eq. (18) into Eq. (31) leads to an equation for current density, i_s [=] (amp / cm_S^2), given by:

$$i_s = \left(FC^S \sqrt{\frac{\bar{D}_e}{\pi t}} \right) \qquad (32)$$

The current density calculated from Eq. (32) should be used in the formulation to compute the kinetic polarization voltage loss associated with the charge transfer across the electrolyte-cathode electrode active material interface [6].

III. COMPUTED DATA AND DISCUSSION

The concentration profile provided by Eq. (14) is shown in Figure 2. This demonstrates the form of the concentration profile at any time, t, for any material with effective diffusivity, $\bar{D}_e$, as η, according to Eq. (9), functions as a position variable. The expected form of experimental data that fits this model can be shown graphically by defining dimensionless time as:

$$\tau = \frac{\bar{D}_e t}{L^2} \qquad (33)$$

The concentration boundary layer thickness can be defined as a dimensionless quantity relative to the total active material thickness, L, by dividing Eq. (16) by L and using Eq. (33) to simplify and obtain:

$$\frac{\delta_C}{L} = 4\sqrt{\tau} \qquad (34)$$

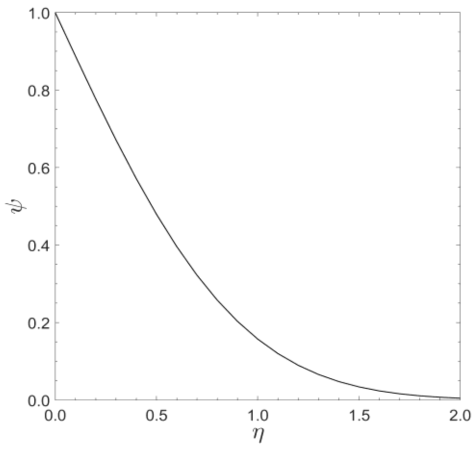

Figure 2: Dimensionless concentration versus lumped parameter, η, based on Eq. (14).

Figure 3 shows the dimensionless concentration boundary layer thickness δ_C / L versus $\sqrt{\tau}$. So long as the thickness, L, and the effective diffusivity, $\bar{D}_e$, are known, Figure 3 is representative of the linear fit that the experimental boundary layer thickness versus time data should fit if the model holds.

The specific charge capacity, Eq. (25), can be redefined as the specific charge capacity per mole of lithium stored in the active material, (mAh/g-mol Li), by multiplying by ρ_{activ} ,dividing by C^S , and using Eq. (33) to simplify:

$$Q_{sp,\tau} = \frac{Q_{sp,t}\rho_{activ}}{C^S} = 3.0243\times 10^4\sqrt{\tau} \qquad (35)$$

Figure 4 shows the linear relationship between specific charge capacity per mole of lithium and the square root of dimensionless time. This linear relationship should describe the experimental data which follows this model.

The fractional utilization, Eq. (30), which is dimensionless by definition, can be rearranged into the following form:

$$f_{ut,\tau,altern} = \frac{f_{ut,t}\rho_{activ}X_{\max}}{C^S M_{activ}} = \left(\frac{2}{\sqrt{\pi}}\right)\sqrt{\tau} \qquad (36)$$

Figure 5 shows the plot of $f_{ut,\tau,altern}$ versus $\sqrt{\tau}$. The linear relation between $f_{ut,\tau,altern}$ and $\sqrt{\tau}$ is obvious. The maximum value of $f_{ut,\tau,altern}$ is 16% while satisfying the requirement for the validity of the boundary condition, Eq. (8).

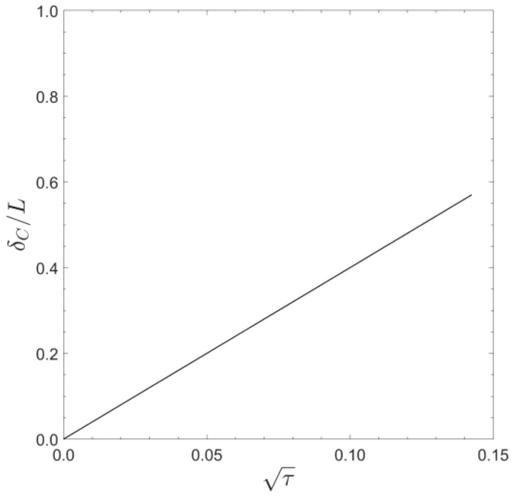

Figure 3: Dimensionless concentration boundary layer thickness versus the square root of dimensionless time.

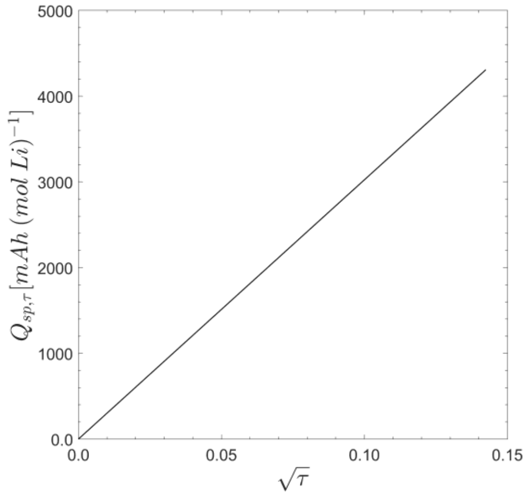

Figure 4: Specific charge storage capacity per mole of lithium intercalated versus the square root of dimensionless time, $\sqrt{\tau}$.

The current density defined in Eq. (32) is re-expressed as the dimensionless current density using the information provided by Eq. (33), in the following form:

$$i_{s,d} = \frac{i_s L}{F\bar{D}_e C^S} = \sqrt{\frac{1}{\pi}}\left(\tau\right)^{-1/2} \qquad (37)$$

Dimensionless current density has an inverse relationship with the square root of dimensionless time, $\left(\tau\right)^{-1/2}$, leading to a decreasing current density with increasing values of τ.

Figure 6 shows the linear relationship when dimensionless current density, $i_{s,d}$, is plotted versus the inverse of the square root of dimensionless time, $(\tau)^{-1/2}$. The value of time, *t*, increases from right to left, corresponding to the decrease in the dimensionless current density.

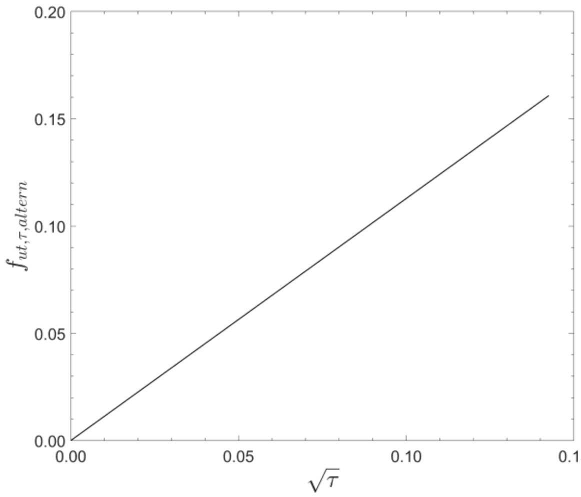

Figure 5: The fractional utilization, $f_{ut,\tau,altern}$, versus the square root of dimensionless time, $\sqrt{\tau}$.

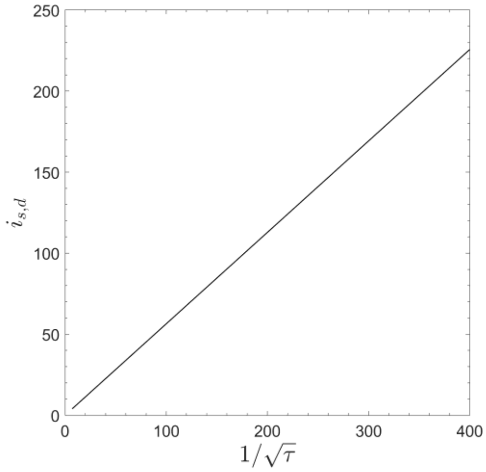

Figure 6: Dimensionless current density versus the inverse of the square root of dimensionless time.

IV. CONCLUSIONS

A mathematical model for the lithium-ion intercalation into the cathode active material (e.g. copper phthalocyanine ($CuPc_{(s)}$) of a lithium-based cell: $Li_{(s)}$/electrolyte/cathode electrode containing $CuPc_{(s)}$, has been developed to provide insight into the performance behavior of such cells currently being investigated in our experimental program on lithium-based cells/batteries. The fact; derived from our previous experimental work on the cells of the type mentioned above; that the diffusion of lithium ions in the cathode active material controls the overall cell discharge process, was used as the basis for the model development for short cell-discharge periods. The one-dimensional model for the slab type geometry of the cathode active material predicts the following:

(a) The transient lithium-ion concentration profile in the cathode active material.
(b) The thickness of the transient lithium-ion concentration boundary layer development in the solid cathode active material proportional to the square root of the cell discharge time.
(c) The dimensionless cell electrolyte – cathode electrode active material interfacial current density which varies inversely with the square-root of dimensionless time.
(d) The transient specific active material charge storage capacity which varies in direct proportion to the square-root of time.
(e) The transient fractional utilization of the cell cathode active material which also varies in direct proportion to the square-root of time.

REFERENCES

1. Sandhu, S.S., Fellner, J.P. (2015), J. Chem. Eng. Process Technol., 6, 257.
2. Sandhu, S.S., Fellner, J.P., Tsao, M., Cashion, C.J. (2017), International Journal of Engineering Technology Management and Applied Sciences (IJETAS), 5, 24.
3. Sandhu, S.S., Fellner, J.P., Dudi, S.P. (2017), Current Topics in Electrochemistry, 19, 91.
4. Froment, G.F., Bischoff, K.B., Wilde, J. De. (2011), Chemical Reactor Analysis and Design (3rd Edition), John Wiley & Sons, Inc., p. 173.
5. Bird, R.B, Stewart, W.E., Lightfoot, E.N. (2007), Transport Phenomena (revised second edition), John Wiley & Sons, Chapters 18 and 19.
6. Sandhu, S.S., Cashion, C.J., Fellner, J.P. (2018), Theoretical and Experimental Characterization of a Rechargeable Hybrid Cathode for Lithium-based Batteries. Paper number 49b published in the Proceedings of 2018 AIChE Annual Meeting, Pittsburgh, Pa., October 28-November 1, 2018. The 2018 Proceedings number: 978-0-8169-1108-0.